Sensors & Actuators: B. Chemical 274 (2018) 194–200

Contents lists available at ScienceDirect

Sensors and Actuators B: Chemical

journal homepage: www.elsevier.com/locate/snb

Selective monitoring of vascular cell senescence via β-Galactosidase detection with a fluorescent chemosensor

Eun-Joong Kim[a,1], Arup Podder[b,1], Mrinmoy Maiti[b], Jong Min Lee[c], Bong Geun Chung[c,*], Sankarprasad Bhuniya[b,d,**]

[a] Research Center, Sogang University, Seoul, 04107, Republic of Korea
[b] Amrita Centre for Industrial Research & Innovation, Amrita School of Engineering, Coimbatore, Amrita Vishwa Vidyapeetham, 641112, India
[c] Department of Mechanical Engineering, Sogang University, Seoul, 04107, Republic of Korea
[d] Department of Chemical Engineering & Materials Science, Amrita School of Engineering, Coimbatore, Amrita Vishwa Vidyapeetham, 641112, India

ARTICLE INFO

Keywords:
β-Galactosidase
Fluorescent probe
Acidic lysosome
Rhodol
Vascular cell senescence

ABSTRACT

A new senescence-responsive fluorescent probe (**SRP**) was developed for the detection of β-galactosidase activity in senescent cells. UV-absorption of t probe **SRP** at 495 nm was increased in the presence of β-galactosidase. Its fluorescence at λ_{em} 545 nm increased ~27-fold upon incubation with β-galactosidase (0.1 U/mL). The **SRP** probe is non-toxic and highly chemoselective for β-galactosidase. The high cell viability and chemoselcivity of probe **SRP** offer it to be a suitable marker for assessing cell senescence in live cells. Using this probe, H_2O_2-induced cellular senescence of human umbilical vein cells (HUVECs) could be distinguished from normal cells based on the extent of fluorescent labeling of the cells. Moreover, it was preferentially localized in acidic lysosomes. Overall, **SRP** is a unique chemosensor that can provide preclinical information on cell senescence in vascular endothelial cells.

1. Introduction

Ageing is associated with the occurrence of various diseases due to the gradual weakening of the normal healthy condition. Age-related diseases are rapidly becoming a burden in both developing and advanced countries because they increase healthcare expenditures, they reduce the quality of life, and the elderly population is greatly increasing throughout the world [1,2]. Notably, the morbidity and mortality rates for vascular disease are higher among the elderly. Vascular ageing is induced by the accumulation of senescent endothelial cells that have less replicative potential, which results in impaired angiogenesis [3–5]. Moreover, cellular senescence is closely related to oxidative stress and telomere shortening, all of which are thought to prevent the progression of cancers [6,7]. Therefore, determining the mechanisms behind vascular ageing or developing a method for identifying senescent cells might provide robust therapeutic targets for treating age-related diseases and for maintaining the ability to protect against cancers.

β-galactosidase (β-Gal), as a representative biomarker for ageing, is highly expressed in senescent endothelial cells [8]. The enzymatic activity of β-Gal cleaves galactose residues from various substrates such as glycoproteins, sphingolipids, and keratansulfates [9,10]. Additionally, its enzymatic activity is confined to the acidic conditions in the lysosomes, and the increased lysosomal content of senescent cells allows β-Gal activity to be detected at pH 6 [11–13]. The use of this property to characterize lysosomal β-Gal activity is critically important for identifying age-induced pathological conditions; thus, a variety of methods for the detection of β-Gal in senescent cells have been developed in the last decade.

Visualization of β-Gal activity has widely been used to monitor its role in various physiological conditions, such as ageing, senescence, and carcinogenesis. A wide range of sensing technologies have been developed to detect β-Gal including cytochemical assays that use the chromogenic substrate, 5-bromo-4-chloro-3-indolyl β-D-galactopyranoside (X-Gal) [14,15], flow cytometric analysis using 5-dodecanoylaminofluorescein di-β-D-galactopyranoside (C12FDG) [11], and various fluorogenic probes using derivatives of resorufin [16], coumarin [17], fluorescein [18,19], and rhodamine [20]. In particular,

* Corresponding author.
** Corresponding author at: Amrita Centre for Industrial Research & Innovation, Amrita School of Engineering, Coimbatore, Amrita Vishwa Vidyapeetham, 641112, India.
E-mail addresses: bchung@sogang.ac.kr (B.G. Chung), b_sankarprasad@cb.amrita.edu (S. Bhuniya).
[1] These authors contributed equally to this work.

https://doi.org/10.1016/j.snb.2018.07.171
Received 10 April 2018; Received in revised form 30 July 2018; Accepted 31 July 2018
Available online 01 August 2018
0925-4005/

fluorescent imaging agents have been regarded as the most effective visualization tool owing to their high sensitivity, reduced invasiveness, and their ability to be assessed in real-time [21–24]. Most fluorescent probes capable of detecting β-Gal were designed to measure its activity and are used for cancer diagnosis, since it is known to be highly expressed in various cancers [25–27]. Moreover, some animal xenograft models and cell culture systems have been used to monitor senescence-associated enzymatic activity in various cancers [28,29]. However, the use of fluorescence imaging to assess vascular endothelial cell senescence has rarely been reported, even though a flow cytometry assay has been used to quantify β-Gal activity in human vein endothelial cells (HUVECs) [11]. Thus, we are interested in developing lysosomal targeted β-Gal for assessing cell-senescence activity in human vein endothelial cells as described in bellow.

Here, we describe a rhodol-based fluorescence probe for the selective detection of lysosomal β-Gal in cellular senescence of vascular endothelial cell. A senescence-specific fluorescent probe, **SRP**, showed low cytotoxicity and was used as a fluorescent tracer in response to endogenous β-Gal activity in H_2O_2-induced senescent HUVECs. In addition, the pH profiles of **SRP** were also confirmed by the measurement of fluorescence intensity at different pH values, quantum yield analysis, and fluorescence-based lysosomal localization study. This fluorescent chemosensor can offer a new modality for fluorescence imaging of the vascular senescent endothelial cell and could be used as a promising novel diagnostic agent for age-related diseases.

2. Material and methods

2.1. General information on materials, methods and instrumentations

tert-Butyl bromoacetate 3-(1-piperazinyl)-phenol (Alfa-Aesar), 2,3,4,6-tetra-O-acetyl-α-D-galactopyranosyl-1-bromide (Sigma-Aldrich), Silver (I) Oxide (Sigma-Aldrich), sodium (Avra), K_2CO_3 (Rankem), MeOH (Mark), TFA (Sigma-Aldrich), acetonitrile (Avra) were purchased commercially and used without further purification. Flash column chromatography was performed using silica gel (100–200 mesh) and analytical thin layer chromatography was performed using silica gel 60 (pre-coated sheets with 0.25 mm thickness). Mass spectra were recorded on anion SpecHiResESI mass spectrometer. NMR spectra were collected on a 400 MHz spectrometer (Bruker, Germany).

2.2. Synthesis of *SRP*

2.2.1. Synthesis *1*

2-(2, 4-Dihydroxybenzoyl) benzoic acid was synthesized in accord with a reported procedure (supplementary information). Yield 72%.

2.2.2. Synthesis *SRP-r*

2-(2, 4-Dihydroxybenzoyl) benzoic acid (**1**, 1.24 g, 4.8 mmol) and 1-(3-hydroxy phenyl)-piperazine (853 mg, 4.8 mmol) were added to a pressure flask and dissolved in 20 mL of TFA. The reaction was stirred for 3 h at 95 °C. After cooling, the reaction mixture was poured into 300 mL of ether. The resulting precipitate was collected, immediately redissolved in methanol and then evaporated to dryness under reduced pressure to yield red solid. The crude product was carried on without further purification. The crude product (1.09 g), tert-butyl bromoacetate (527 mg, 2.7 mmol) and K_2CO_3 (1.12 mg, 8 mmol) were added to a round bottom flask. Then 20 mL of acetonitrile was added and then stirred the reaction mixture at 85 °C for 12 h. Then the product was extracted into ethyl acetate, washed with water and dried under reduced pressure. Purification by column chromatography (1:1 hexane/ethyl acetate) provided ***SRP*-r** as a red solid (1 mg, 42% overall yield). ^{1}H-NMR (400 MHz, DMSO-d_6): δ 8.035 (d, J = 6.4 Hz, 1 H); 7.636 (m, 2 H); 7.578 (m, 1 H); 7.162 (d, J = 6.8 Hz, 1 H); 6.726 (d, J = 2 Hz, 2 H); 6.703 (s, 1 H); 6.610 (d, J = 2.4 Hz, 2 H); 6.520 (d, J = 2.4 Hz, 1 H); 3.277 (s, 3 H); 3.217 (s, 3 H); 2.766 (s, 4 H); 1.406 (s, 9 H). ^{13}C-NMR (100 MHz, DMSO-d_6): δ 169.166, 168.702, 159.440, 152.465, 139.946, 132.116, 129.994, 128.278, 126.223, 124.531, 123.984, 113.277, 111.672, 109.672, 108.152, 102.469, 101.039, 80.206, 69.166, 59.080, 56.080, 51.539, 47.266, 27.786. ESI-HRMS m/z (M + H) calcd.515.21039, found: 515.21704.

2.2.3. Synthesis *A*

SRP-r (514 mg, 1 mmol), tetra-O-acetyl-α-D-galacto-pyranosyl-1-bromide (452 mg, 1.1 mmol), Ag_2O (440 mg, 1.9 mmol) and 15 mL Acetonitrile were added in a 50 mL r.b and stirred this reaction mixture for 48 h under nitrogen atmosphere at r.t. TLC was checked and then filtered. Then filtrate was evaporated to dryness. Purification was done by column chromatography (20% hexane in ethylacetate) to get **A** (700 mg, 82% yield).^{1}H-NMR (400 MHz, DMSO-d_6): δ 8.009 (d, J = 7.6 Hz, 1 H); 7.762 (m,1 H); 7.718 (td, 1 H); 7.252 (m, 1 H); 7.161 (d, J = 4.8 Hz, 1 H); 6.975 (s, 1 H); 6.740 (m, 4H); 6.555 (m, 1H); 5.360 (d, J = 3.2 Hz, 1 H); 5.262 (m, 1 H); 5.122 (m, 1 H); 4.905 (dd, J = 10.4, 2.8 Hz, 1 H); 4.492 (t, J = 6 Hz, 1 H); 4.385 (m, 1 H); 3.291 (s, 6 H); 2.620 (s, 4 H); 2.145 (m, 9 H); 2.098 (s, 3 H); 1.407 (s, 9 H). ^{13}C-NMR (100 MHz, DMSO-d_6): δ 169.180, 168.575, 157.790, 152.275, 135.633, 129.311, 128.301, 126.036, 124.026, 113.237, 112.010, 107.813, 103.366, 100.789, 97.319, 94.205, 91.265, 89.421, 82.408, 80.232, 70.550, 68.137, 65.291, 61.825, 59.040, 51.514, 47.198, 27.780. ESI-HRMS m/z (M + H) calcd. 845.30547, found: 845.31171; m/z (M^+Na^+) calcd. 867.29469; found: 867.31281.

2.2.4. Synthesis *SRP*

Compound **A** (0.36 g, 0.42 mmol) was dissolved in methanol (6 mL) under nitrogen gas. 0.5 N sodium methoxide (0.4 mL) in methanol was added in the solution. The mixture was magnetically stirred in the dark for 3 h at room temperature. DOWEX 50wx8 50–100 (H), Cation-exchange resin (H^+) was added and filtered and washed with MeOH. The solvent was evaporated *in vacuo* to get **SRP** (200 mg, 69% yield). ^{1}H-NMR (400 MHz, DMSO-d_6): 8.002 (d, J = 7.6 Hz,1 H); 7.800 (t,7.6 6 Hz, 1 H); 7.730 (t,7.6 6 Hz, 1 H); 7.297 (d, 8 Hz, 1 H); 6.959 (s, 1 H); 6.751 (m, 4 H); 6.663 (d, 8 Hz, 1 H); 6.526 (d, J = 8.8, 2 Hz, 1 H); 5.165 (q, J = 5.2 Hz, 1 H); 4.910 (m, 1 H); 4.851 (q, J = 6 Hz, 1 H); 4.670 (t, J = 5.2 Hz, 1 H); 4.501 (d, J = 4.8 Hz, 1 H); 3.706 (s, 1 H); 3.599 (d, J = 6 Hz, 1 H); 3.513 (m, 2 H); 3.416 (m, 1 H); 3.226 (s, 4 H); 3.148 (s, 2 H); 2.624 (d, J = 3.6 Hz, 4 H); 1.406 (s, 9 H). ^{13}C-NMR (100 MHz, DMSO-d_6): δ 169.179, 168.662, 159.025, 152.467, 151.737, 135.596, 131.536, 130.113, 128.332, 126.058, 124.623, 123.973, 113.138, 112.272, 107.880, 103.266, 100.800, 82.749, 80.203, 75.655, 73.177, 70.110, 68.085, 59.083, 51.543, 47.248, 28.978. HRMS m/z (M + H) calcd. 677.26321, found 677.27008; m/z (M + Na+) calcd. 699.25243; found: 699.25189.

2.3. UV–vis and fluorescence spectroscopy

Stock solution (2×10^{-5} M) of the probe was prepared by dissolving probe in DMSO. Absorption spectra were recorded on an S-3100 (Scinco) spectrophotometer, and fluorescence spectra were recorded using an RF-6500 PC Spectrofluorometer (Shimadzu) fitted with a xenon lamp. The fluorescence emission spectra were recorded at excitation wavelength of 495 nm and emission was monitored over wavelength the range of 500–700 nm (λ_{em} = 545 nm). The stock solutions of various analytes (100 μM) a) GSH; b) cysteine; c) pepsin; d) trypsin; e) NO; f) α-gal; g) H2S; h) H_2O_2; i) NaOCl; *j*) NADH; k) S_2O_3; l) HNO; m) phosphatase; n) β-galactosidase (0.1U) in distilled water; and ALP was prepared in HEPES buffer (0.1 M). Quartz cuvettes were used for absorption and emission measurements (4 mL volume) of samples. All spectroscopic measurements were performed under physiological (HEPES buffer, pH 7.4) and acidic (HEPES buffer, pH 6.0) conditions of pH.

2.4. Cell culture and cytotoxicity

The HUVEC cells were cultured on a 2% gelatin-coated with endothelial cell growth medium (EGM-2, Lonza, Switzerland) supplemented with 10% fetal bovine serum (FBS, Gibco, CA, USA) and 1% penicillin/streptomycin (Gibco) in an incubator (5% CO_2, 37 °C). The cells were seeded into each well of 96 well plates at 1×10^4 cells/well, and were treated with **SRP** at various concentrations for 24 h. Then, cytotoxicity was assessed by a 3-(4,5-dimethylthiazol-2-yl)-2,5-diphenyl tetrazolium bromide (MTT, Roche Diagnostics GmbH, Mannheim, Germany). After washing with PBS, 10 µL of MTT reagent was added into each well and incubated for an additional 4 h. Following the addition of solubilization buffer (Roche Diagnostics) to each well, the absorbance of MTT formazan product was determined at 570 nm using a microplate reader (EL800, Bio-Tek Instruments, Winooski, VT, USA).

2.5. Fluorescence imaging under senescent condition

For fluorescence imaging, the premature senescence was initially induced by the treatment of H_2O_2 (Sigma, St. Louis, MO, USA). The HUVEC cells were plated at 1×10^5 cells/mL suspension in μ -slide 8 well (ibidi, Munich, Germany) and allowed to culture overnight. Then the cells were treated with 150 µM H_2O_2 for 2 h with fresh culture medium, followed by further incubation with 10 µM H_2O_2 for 24 h after resuspending in phosphate-buffered saline (PBS) three times [30,31]. Normal HUVEC cells untreated with H_2O_2 were used as controls. Next, 50 µM of **SRP** was added into both HUVEC cell groups for 24 h. After washing in PBS, cells were fixed in 4% paraformaldehyde, and stained with DAPI (Invitrogen, Molecular Probe, Eugene, OR, USA), Alexa Fluor 488 phalloidin (Invitrogen, Molecular Probe), LysoTracker green (Invitrogen, Molecular Probe) for nuclear, actin filaments, and lysosomes staining, respectively. The fluorescent cell images were obtained by a confocal imaging microscope (LSM 710, Carl Zeiss, Germany). To detect β-gal activity in senescent HUVECs, X-gal staining was conducted using a commercially available Senescence β-Galactosidase Staining Kit (Cell Signaling Technology, Danvers, MA, USA), according manufactures instructions. Images of senescent HUVECs by X-gal staining were acquired using a fluorescent microscope (IX37, Olympus, Japan).

3. Results and discussion

3.1. Synthesis and photophysical properties

The **SRP** probe was synthesized in three successive steps (Scheme 1). First, rhodol was prepared as previously described [32] and was subsequently reacted with tert-butyl bromoacetate to produce **SRP-r**. Next, **SRP-r** was reacted with tetra-O-acetyl-α-D-galacto-pyranosyl-1-bromide in the presence of Ag_2O as a catalyst to yield compound **A**, which was hydrolyzed to produce the **SRP**. The details of the synthesis method are provided in the experimental section. The chemical structure of each new compound (**SRP-r**, **A**, **SRP**) was elucidated by ^{1}H-NMR, ^{13}C-NMR, and HRMS analyses (Figs. S5–S13).

The new **SRP** was used to detect β-Gal under artificial physiological conditions. As shown in Fig. S1, UV-absorption by the **SRP** at λ_{abs} 495 nm increased ~2-fold after incubation with β-Gal (0.1 U) for 30 min. Fluorescence spectroscopy showed that the emission of the **SRP** at λ_{em} 545 nm increased continuously with exposure to increasing concentrations of β-Gal (0 - 0.1 U) in buffer at acidic pH 6.0 (Fig. 1a) which is referred to be a lysosomal senescence. Ultimately, an ~27-fold increase in fluorescence intensity was detected in the presence of 0.1 U of β-Gal. Applying regression equation, the lower detection limit was found to be 4.19×10^{-7} U (Fig. S2). Next, the amount of β-Gal that was consumed by the **SRP** over time was determined. This experimental result provides information on the temporal activity of the probe towards β-Gal. As shown in Fig. 1b, the fluorescence emission of the **SRP** concomitantly increased with time and plateaued within 30 min. These results support the high reactivity of the **SRP** towards β-Gal. and enhanced fluorescence in an acidic environment.

To explore the chemo-selectivity of the probe **SRP** for β-Gal compared to other biologically relevant analytes, we studied the fluorescence of the **SRP** in the presence of various analytes. The results depicted in Fig. 2a indicate that the fluorescence of the **SRP** did not change in the presence of other analytes including GSH, Cys, pepsin, trypsin, ALP, α-Gal and others. From this result we conclude that the probe is highly chemo-selective for β-galactosidase and that it can be used to detect cell senescence in living cells.

Since our goal is to detect β-Gal activity in acidic lysosomes, we analyzed the reactivity of the **SRP** with β-Gal over a range of pH values. As shown in Fig. 2b, the fluorescence intensity of the **SRP** increased at lower pH values (≤5.0) compared to its intensity at an alkaline pH (≥7.0). Thus, at pH 6.0 the quantum yield (Φ) of the **SRP** increased from 0.037 to 0.553 (Table S1) upon exposure to β-Gal (0.1 U). Moreover, we noticed fluorescence intensity variation of β-Gal pretreated **SRP** within a pH scale 5–9 is similar with **SRP-r**, it implied that the reactivity of **SRP** toward β-Gal is same irrespective of the pH; however fluorescence intensity changes with the pH because of the fluorophore (**SRP-r**) responses to the pH (Fig. S3). From this experimental result, we envisioned that the **SRP** could detect β-Gal activity in the lysosomes of senescent cells.

Also, we have determined the kinetics of the enzymatic hydrolysis reaction by assaying various kinetic parameters including Michaelis

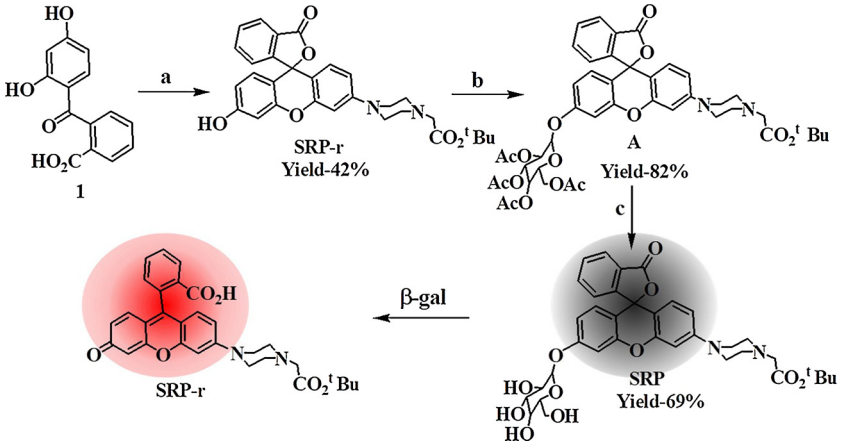

Scheme 1. Reaction scheme for **SRP** synthesis. **a**: 1-(3-hydroxy phenyl)-piperazine, TFA, 95 °C, 3 h; then, $BrCH_2CO_2tBu$, K_2CO_3, ACN, 85 °C,12 h; **b**: tetra-O-acetyl-α-D-galactopyranosyl-1-bromide, Ag_2O, ACN, rt, 48 h; **c**: NaOMe, MeOH, 2 h, rt.

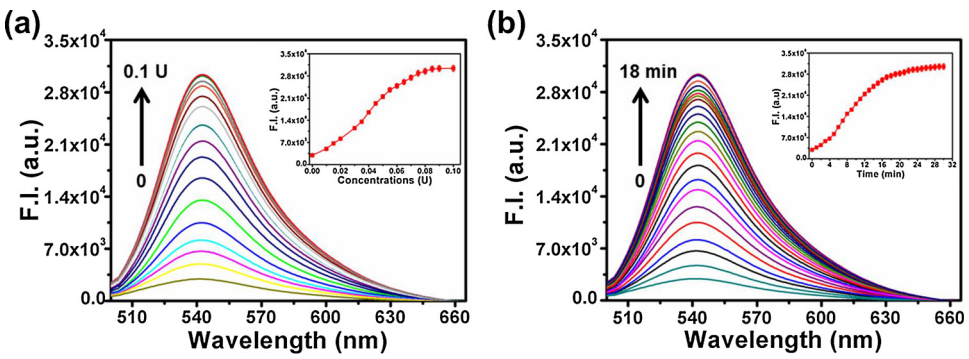

Fig. 1. (a) Fluorescence study of the **SRP** (5.0 μM) with β-Gal (0–0.1U) at pH 6.0 in HEPES buffer solution (0.5% DMSO in HEPES) at 37 °C. All the data were acquired 30 min after addition of β-Gal at 37 °C. (b) Fluorescence time-course study of the **SRP** (5.0 μM) with 0.1U of β-Gal at pH 6.0 in HEPES buffer solution (0.5% DMSO in HEPES). The excitation and emission wavelengths were 495 nm and 545 nm, respectively. The excitation and emission slit widths were both set at 5 nm.

constant (K_M), the catalytic efficiency constant (k_{cat}/K_M), and the turnover number (k_{cat}). For this, we examined the time-dependent fluorescence intensity increment at 545 nm at a fixed concentration of β-gal (0.02 U) with variable concentrations of **SRP** (0–20 μM). We found that the rate of reaction was increased along with increasing concentrations of **SRP** (Fig. S4). Applying Michaelis-Menten and Lineweaver–Burk equation, [33] K_M, k_{cat}, V_{max} and k_{cat}/K_M were found to be 28.0 μM, $1.25 \times 10^3 s^{-1}$, 25 μM s^{-1} and 4.5×10^7 $M^{-1}s^{-1}$ respectively. The value of k_{cat}/K_M of **SRP** indicates that **SRP** is highly reactive toward β-gal.

3.2. Cytotoxicity evaluation

To determine the appropriate concentration of the **SRP** to use for fluorescence imaging of senescent endothelial cells, its cytotoxicity was assessed. Cell viability was initially evaluated by an MTT colorimetric assay. As shown in Fig. 3, HUVECs were treated with different concentrations of the **SRP** for 24 h and were subsequently assessed by MTT analysis. Viability values over 80% were consistently observed even when incubated with high concentrations (100 μM) of the **SRP**, indicating that it had good biocompatibility. A 50 μM concentration of the SRP that exhibited a relatively low cytotoxicity was used for the remaining experiments.

3.3. Fluorescence imaging in senescent vascular cell line

The intracellular fluorescence of the **SRP** in response to β-Gal was assessed by comparing its fluorescence in normal and senescent HUVECs (Scheme 2). To evaluate the capabilities of the **SRP** and its applicability in the fluorescence-based detection of β-Gal, cellular senescence was induced by treating HUVECs with hydrogen peroxide (H_2O_2) [30,31]. Intracellular

senescent conditions were confirmed calorimetrically by staining

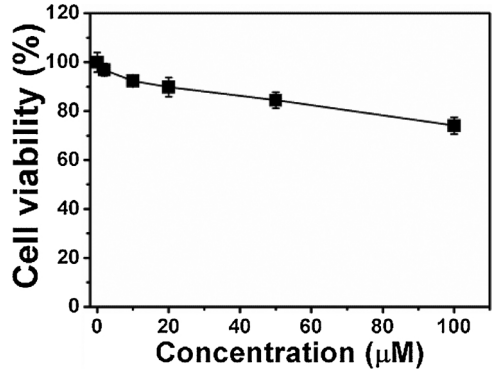

Fig. 3. Cell viability of **SRP** in HUVEC cells. HUVEC cells were incubated with various concentrations of **SRP** for 24 h and cell viability was measured using a MTT assay.

with commercial X-gal (Fig. 4a). After treatment with a 50 μM concentration of the **SRP** for 24 h (a concentration with relatively low cytotoxicity), the fluorescence was significantly increased in the H_2O_2-induced senescent environment, while less intense fluorescence was observed in the normal control HUVECs (Fig. 4b). This observation was quantitatively supported by analysis with ImageJ software (Fig. 4c). Moreover, when normal and H_2O_2-induced senescent HUVECs were treated with the control compound **SRP-r** (Φ = 0.65, Table S1), which lacks a galactose residue, almost same fluorescence was observed in both HUVECs regardless of senescent condition (Fig. 5). The fluorescence signal in senescent cells indicated that the **SRP** could specifically identify β-Gal activity for the detection of vascular cell senescence.

3.4. Co-localization with lysosomes

Based on previous reports that β-Gal accumulates and is activated in

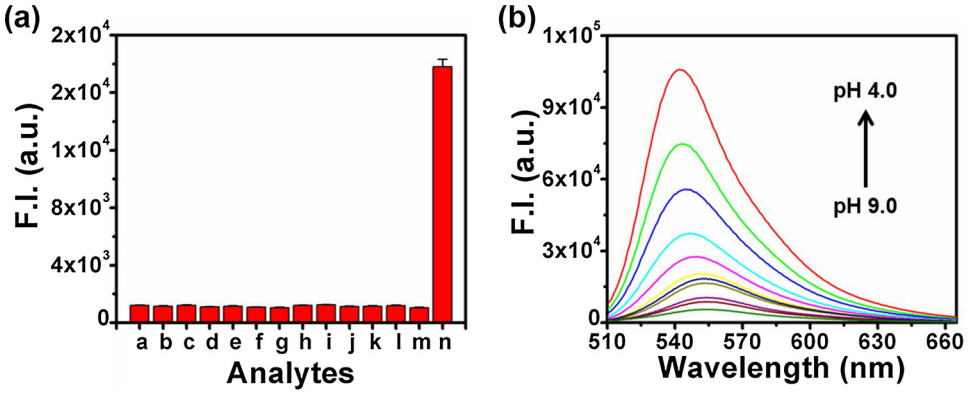

Fig. 2. (a) Tests of various analytes (100 μM) with the **SRP** (5.0 μM). a) GSH; b) Cys; c) pepsin; d) tripsin; e) NO; f) α-Gal; g) H_2S; h) H_2O_2; i) NaOCl; j) NADH; k) S_2O_3; l) phosphatase (ALP); m) HNO; and n) β-Gal (0.1U) at pH 6.0 in HEPES buffer solution (0.5% DMSO in HEPES buffer) at 37 °C. (b) Comparative fluorescence study of the **SRP** (5.0 μM) with 0.1U of β-Gal over a range of pH values (5.0–9.0) in HEPES Buffer solution (0.5% DMSO in HEPES) at 37 °C. All the data were acquired 30 min after addition of β-Gal at 37 °C. The excitation and emission wavelengths were 495 nm and 545 nm, respectively. The excitation and emission slit widths were both set at 5 nm.

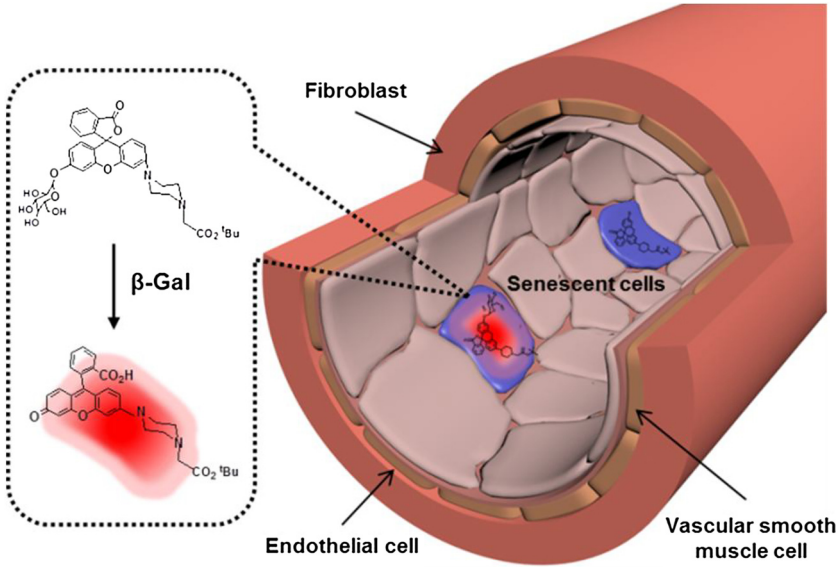

Scheme 2. Schematic illustration of the monitoring of SRP fluorescence in senescent vascular endothelial cells.

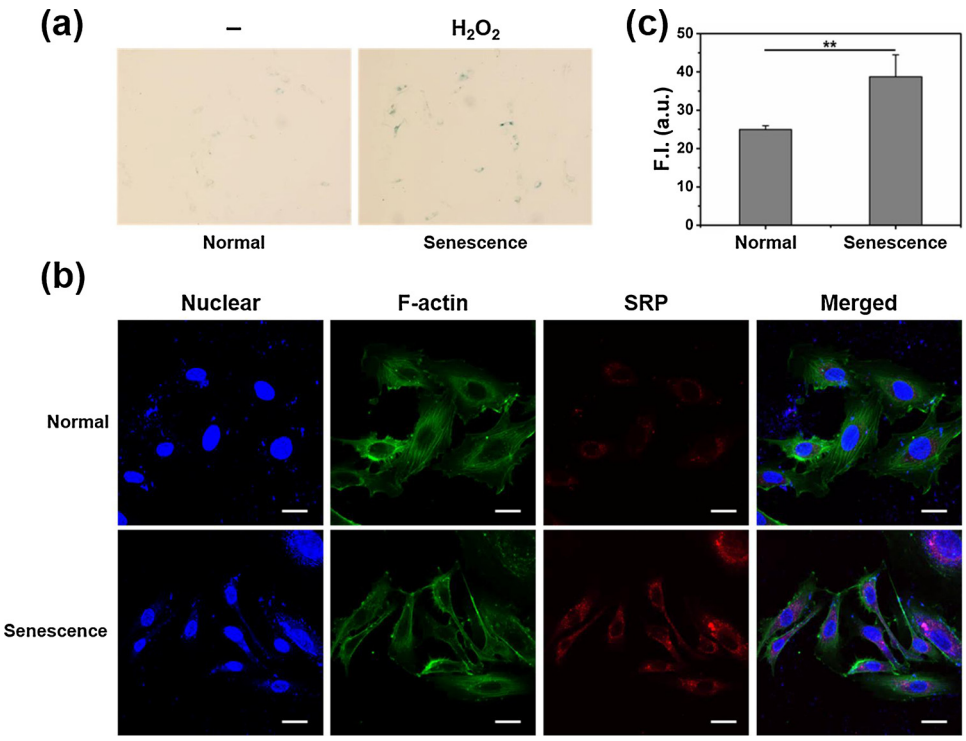

Fig. 4. (a) Cytochemical staining of β-gal. Activity in normal HUVECs and senescent HUVEC cells induced by H_2O_2 treatment. (b) Fluorescence images of HUVECs treated with the **SRP** under normal and senescent conditions. HUVECs were treated with 50 μM **SRP** for 24 h. Filter sets: **SRP** (Red, λ_{ex}: 512/λ_{em}: 552), F-actin (λ_{ex}: 495 / λ_{em}: 518 and DAPI (λ_{ex}: 358 / λ_{em}: 461) Scale bar: 20 μm. (c) Mean fluorescence intensity was analyzed using ImageJ software at normal or senescent HUVEC cells (5 cells per each group) treated with **SRP** at a concentration of 50 μM. (**$p < 0.01$) (For interpretation of the references to colour in this figure legend, the reader is referred to the web version of this article.).

lysosomes, we evaluated whether the **SRP** co-localized with lysosomal position and exhibited intense fluorescence at low pH. HUVECs were incubated with the **SRP** for 24 h and then stained with a lysosome-specific fluorescent dye. As shown in Fig. 6, a strong fluorescence signal from the **SRP** was found to be mainly co-localized in organelle lysosomes and provided complementary images, but not in the nucleus. Such extent of colocalization strongly suggested Pearson's coefficient value should be ≥0.90 [33,34]. This co-localization result concurred with the fluorescence spectral profiles and quantum yield of the **SRP** at different pH values, suggesting that the fluorescence from activation of the **SRP** could be selectively induced by β-Gal activity in the acidic pH of the lysosomal- environment in ageing HUVECs.

4. Conclusions

We described the synthesis and application of a new senescence-specific fluorescent probe, **SRP**. This **SRP** is highly chemoselective and its fluorescence intensity increased 27-fold upon incubation with β-Gal for 30 min under physiological conditions. The fluorescence profile of the **SRP** over a range of pH values confirms that the **SRP** is a potentially powerful candidate for detecting β-Gal expression in the acidic microenvironment. The **SRP** exhibits high cell viability, which makes it suitable for evaluating β-Gal levels in lysosomes with minimal perturbation. After incubation with the **SRP**, the amount of fluorescence labeling in HUVECs in an artificially induced senescent state increased compared to that in normal HUVECs. Its co-localization with lysotracker indicates that the **SRP** is capable of tracking β-Gal, a primary

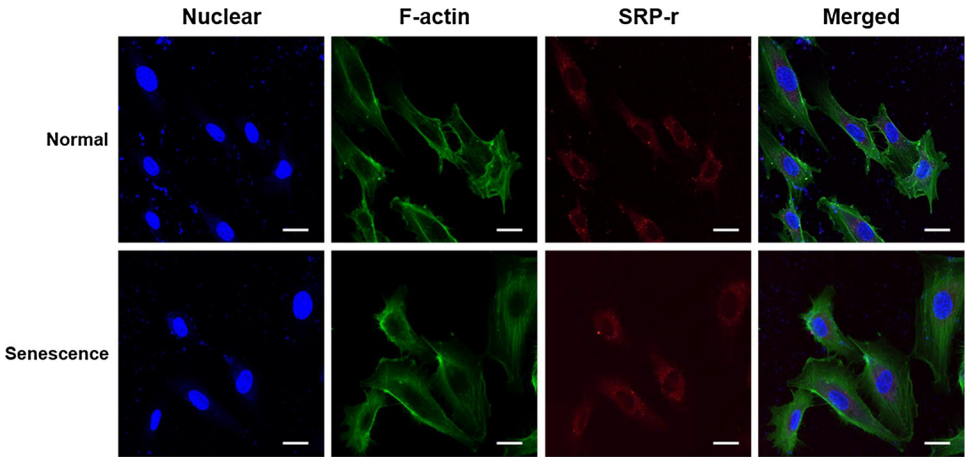

Fig. 5. Fluorescence images of HUVECs treated with the SRP-r under normal and senescent conditions. HUVECs were treated with 50 μM **SRP–r** for 24 h. Filter sets: **SRP-r** (Red, λ_{ex}: 512/λ_{em}: 552), F-actin (λ_{ex}: 495 / λ_{em}: 518 and DAPI (λ_{ex}: 358 / λ_{em}: 461) Scale bar: 20 μm (For interpretation of the references to colour in this figure legend, the reader is referred to the web version of this article.).

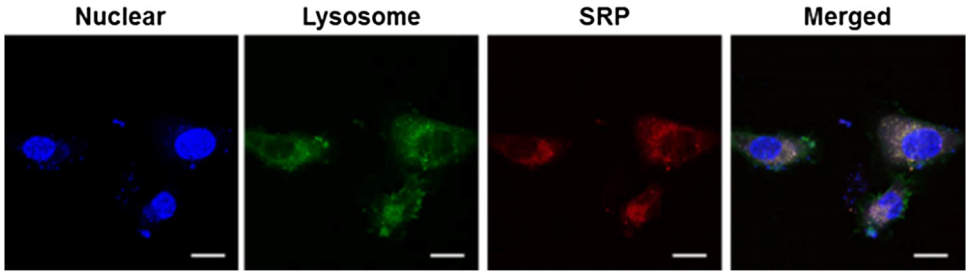

Fig. 6. Co-localization of the **SRP** with lysosomes in HUVECs under senescent conditions. Filter sets: **SRP** (λ_{ex}: 512 / λ_{em}: 552), LysoTracker (λ_{ex}: 504 / λ_{em}: 511 and DAPI (λ_{ex}: 358 / λ_{em}: 461) Scale bar: 20 μm.

contributor to vascular endothelial cell aging. Therefore, this **SRP** provides a new fluorescence imaging method for senescent vascular endothelial cells and could be a promising novel diagnostic agent for age-related diseases.

Acknowledgements

SB thanks DST-SERB, India, for the research grant (ECR/2015/000035). This work is supported by the National Research Foundation funded by the Ministry of Science and ICT (Grant number 2017R1D1A1B04033453, E.J.K). This research was also supported by BioNano Health-Guard Research Center funded by the Ministry of Science and ICT of Korea as Global Frontier Project (Grant number H-GUARD_2013M3A6B2078950 (2014M3A6B2060302), B.G.C). We thank Mr. Jang Ho Ha for drawing the graphical abstract.

Appendix A. Supplementary data

Supplementary material related to this article can be found, in the online version, at doi:https://doi.org/10.1016/j.snb.2018.07.171.

References

[1] T. Niccoli, L. Partridge, Ageing as a risk factor for disease, Curr. Biol. 22 (2012) 741–752.
[2] D. McHugh, J. Gil, Senescence and aging: causes, consequences, and therapeutic avenues, J. Cell Biol. 217 (2018) 65–67.
[3] J. Moriya, T. Minamino, Angiogenesis, cancer, and vascular aging, Front. Cardiovasc. Med. 4 (2017) 65.
[4] Y.T. Ghebre, E. Yakubov, W.T. Wong, P. Krishnamurthy, N. Sayed, A.G. Sikora, M.D. Bonnen, Vascular aging: implications for cardiovascular disease and therapy, Transl. Med. 4 (2016) 183.
[5] P. Mistriotis, S.T. Andreadis, Vascular aging: molecular mechanisms and potential treatments for vascular rejuvenation, Ageing Res. Rev. 37 (2017) 94–116.
[6] X.L. Tian, Y. Li, Endothelial cell senescence and age-related vascular diseases, J. Genet. Genomics 41 (2014) 485.
[7] D. Muñoz-Espín, M. Serrano, Cellular senescence: from physiology to pathology, Nat. Rev. Mol. Cell Biol. 15 (2014) 482–496.
[8] G.P. Dimri, X. Lee, G. Basile, M. Acosta, G. Scott, C. Roskelley, E.E. Medrano, M. Linskens, I. Rubelj, O. Pereira-Smith, A biomarker that identifies senescent human cells in culture and in aging skin in vivo, Proc. Natl. Acad. Sci. U. S. A. 92 (1995) 9363–9367.
[9] G. Noppe, P. Dekker, C.D. Koning-Treurniet, J. Blom, D.V. Heemst, R.W. Dirks, H.J. Tanke, R.G. Westendorp, A.B. Maier, Rapid flow cytometric method for measuring senescence associated beta-galactosidase activity in human fibroblasts, Cytometry A 75 (2009) 910–916.
[10] T. Komatsu, Y. Urano, Evaluation of enzymatic activities in living systems with small-molecular fluorescent substrate probes, Anal. Sci. 31 (2015) 257–265.
[11] D.J. Kurz, S. Decary, Y. Hong, J.D. Erusalimsky, Senescence-associated (beta)-galactosidase reflects an increase in lysosomal mass during replicative ageing of human endothelial cells, J. Cell. Sci. 113 (2000) 3613–3622.
[12] D.J.B. Bernardes, M.A. Blasco, Assessing cell and organ senescence biomarkers, Circ. Res. 111 (2012) 97–109.
[13] K. Itahana, Y. Itahana, G.P. Dimri, Colorimetric detection of senescence-associated β galactosidase, Methods Mol. Biol. 965 (2013) 143–156.
[14] G.P. Dimri, X. Lee, G. Basile, M. Acosta, G. Scott, C. Roskelley, E.E. Medrano, M. Linskens, I. Rubelj, O. Pereira-Smith, A biomarker that identifies senescent human cells in culture and in aging skin in vivo, Proc. Natl. Acad. Sci. U. S. A. 92 (1995) 9363–9367.
[15] V.D. Loo, M.J. Fenton, J.D. Erusalimsky, Cytochemical detection of a senescence-associated beta-galactosidase in endothelial and smooth muscle cells from human and rabbit blood vessels, Exp. Cell Res. 241 (1998) 309–315.
[16] Y. Zhang, W. Chen, D. Feng, W. Shi, X. Li, H. Ma, A spectroscopic off-on probe for simple and sensitive detection of carboxylesterase activity and its application to cell imaging, Analyst 137 (2012) 716–721.
[17] P. Babiak, J.L. Reymond, A high-throughput, low-volume enzyme assay on solid support, Anal. Chem. 77 (2005) 373–377.
[18] Y. Urano, M. Kamiya, K. Kanda, T. Ueno, K. Hirose, T. Nagano, Evolution of fluorescein as a platform for finely tunable fluorescence probes, J. Am. Chem. Soc. 127 (2005) 4888–4894.
[19] L. Tian, Y. Yang, L.M. Wysocki, A.C. Arnold, A. Hu, B. Ravichandran, S.M. Sternson, L.L. Looger, L.D. Lavis, Selective esterase-ester pair for targeting small molecules with cellular specificity, Proc. Natl. Acad. Sci. U. S. A. 109 (2012) 4756–4761.
[20] D. Asanuma, M. Sakabe, M. Kamiya, K. Yamamoto, J. Hiratake, M. Ogawa, N. Kosaka, P.L. Choyke, T. Nagano, H. Kobayashi, Y. Urano, Sensitive β-galactosidase-targeting fluorescence probe for visualizing small peritoneal metastatic tumours in vivo, Nat. Commun. 6 (2015) 6463.
[21] T. Ueno, T. Nagano, Fluorescent probes for sensing and imaging, Nat. Methods 8 (2011) 642–645.
[22] S. Maiti, N. Park, J.H. Han, H.M. Jeon, J.H. Lee, S. Bhuniya, C. Kang, J.S. Kim, Gemcitabine-coumarin-biotin conjugates: a target specific theranostic anticancer prodrug, J. Am. Chem. Soc. 135 (2013) 4567–4572.
[23] D. Dutta, S.M. Alex, K.N. Bobba, K.K. Maiti, S. Bhuniya, New insight into a cancer

theranostic probe: efficient cell-specific delivery of SN-38 guided by biotinylated poly(vinyl alcohol), ACS Appl. Mater. Interfaces 8 (2016) 33430–33438.
[24] B.K. Naidu, G. Saranya, S.M. Alex, N. Velusamy, K.K. Maiti, S. Bhuniya, SERS-active multi-channel fluorescent probe for NO: guide to discriminate intracellular biothiols, Sens. Actuators B Chem. 260 (2018) 165–173.
[25] E.J. Kim, R. Kumar, A. Sharma, B. Yoon, H.M. Kim, H. Lee, K.S. Hong, J.S. Kim, In vivo imaging of β-galactosidase stimulated activity in hepatocellular carcinoma using ligand-targeted fluorescent probe, Biomaterials 122 (2017) 83–90.
[26] G. Jiang, G. Zeng, W. Zhu, Y. Li, X. Dong, G. Zhang, X. Fan, J. Wang, Y. Wu, B.Z. Tang, A selective and light-up fluorescent probe for β-galactosidase activity detection and imaging in living cells based on an AIE tetraphenylethylene derivative, Chem. Commun. 53 (2017) 4505–4508.
[27] A. Sharma, E.J. Kim, H. Shi, J.Y. Lee, B.G. Chung, J.S. Kim, Development of a theranostic prodrug for colon cancer therapy by combining ligand-targeted delivery and enzyme-stimulated activation, Biomaterial 155 (2018) 145–151.
[28] L. Peng, M. Gao, X. Cai, R. Zhang, K. Li, G. Feng, A. Tong, B. Liu, A fluorescent light-up probe based on AIE and ESIPT processes for β-galactosidase activity detection and visualization in living cells, J. Mater. Chem. B 3 (2015) 9168–9172.
[29] B. Lozano-Torres, I. Galiana, M. Rovira, E. Garrido, S. Chaib, A. Bernardos, D. Muñoz-Espín, M. Serrano, R. Martínez-Máñez, F. Sancenón, An OFF-ON two-photon fluorescent probe for tracking cell senescence in vivo, J. Am. Chem. Soc. 139 (2017) 8808–8811.
[30] J. Zhang, C. Li, C. Dutta, M. Fang, S. Zhang, A. Tiwari, T. Werner, F.T. Luo, H. Liu, A novel near-infrared fluorescent probe for sensitive detection of β-galactosidase in living cells, Anal. Chim. Acta 968 (2017) 97–104.
[31] Z. Song, Y. Liu, B. Hao, S. Yu, H. Zhang, D. Liu, B. Zhou, L. Wu, M. Wang, Z. Xiong, C. Wu, J. Zhu, X. Qian, Ginsenoside Rb1 prevents H2O2-induced HUVEC senescence by stimulating sirtuin-1 pathway, PLoS ONE 9 (2014) e112699.
[32] Y. Zhou, K.N. Bobba, X.W. Lv, D. Yang, N. Velusamy, J.F. Zhang, S. Bhuniya, A biotinylated piperazine-rhodol derivative: a' turn-on' probe for nitroreductase triggered hypoxia imaging, Analyst 142 (2017) 345–350.
[33] A. Podder, S. Senapati, P. Maiti, D. Kamalraj, S.S. Jaffer, S. Khatun, S. Bhuniya, A 'turn-on' fluorescent probe for lysosomal phosphatase: a comparative study for labeling of cancer cells, J. Mater. Chem. B Mater. Biol. Med. 6 (2018) 4514–4521.
[34] A. Ji, Y. Fan, W. Ren, S. Zhang, H.-W. Ai, A sensitive near-infrared fluorescent sensor for mitochondrial hydrogen sulfide, ACS Sens. 3 (2018) 992–997.

Eun-Joong Kim is the principal researcher at the Research Center in Sogang University, Seoul, Korea. He obtained his Ph.D. from the Department of Pharmacy at Seoul National University, Korea in 2010. His research interests include the stimuli-responsive activatable systems for therapy, imaging / biochip modalities for diagnosis and monitoring, and advanced cell and gene therapy.

Arup Podder completed his M.Sc. in Chemistry. Currently he is perusing his Pd.D. under the guidance of Prof. Sankarprasad Bhuniya at Amrita Vishwa Vidyapeetham.

Mrinmoy Maiti completed his M.Sc. in Chemistry. Currently he is perusing his Pd.D. under the guidance of Prof. Sankarprasad Bhuniya at Amrita Vishwa Vidyapeetham.

Jong Min Lee received his B.S. degree in Biochemical Engineering from Korea Polytechnic University, Korea in 2010, respectively. In 2016, he received his M.S. and Ph.D. degree in Mechanical Engineering, both from Sogang University, Korea. Currently, he is a research professor for the Department of Mechanical Engineering at Sogang University, Seoul, Korea. His current research interests are development of microfluidic sensing devices for healthcare and medical applications.

Bong Geun Chung received the B.S. and M.S. degree from Hanyang University, Seoul, Korea. In 2007, he obtained Ph.D. degree from Materials Science Engineering in University of California Irvine, USA. After Ph.D. degree, he worked as a Postdoctoral Research Fellow and an Instructor in Harvard Medical School, USA. Currently, he is an Associate Professor at Department of Mechanical Engineering in Sogang University, Seoul, Korea. His main research interests are development of functional 3D Lab-on-a-Chips, Biosensors, and Nanomaterials to direct the stem cell and cancer fate.

Sankarprasad Bhuniya received his M. Sc in chemistry and Ph.D. from IIT Kharagpur India. He spent five years in various chemical and pharmaceutical indus-tries in India. He did a postdocs in POSTECH, South Korea and IIT-Chicago, USA. He also worked as Research Professor at Korea University and KBSI, South Korea 2009-2013. He is a recipient of the Brain Pool Fellow (2018), Korea National Foundation.. He joined Amrita Vishwa Vidyapeeth, India as Research Professor and is leading an independent research group since October 2014. His primary research interests are theranostics, MR-contrast agent development, image-guided drug delivery, and fluorescent probe development.